scientific reports

Check for updates

OPEN

Controlled induction of type 2 diabetes in mice using high fat diet and osmotic-mini pump infused streptozotocin

Emily H. Attrill, Oscar Scharapow, Sathya Perera, Sophie Mayne, Nicole Sumargo, Renee M. Ross, Stephen M. Richards, Brad A. Sutherland & Dino Premilovac✉

Type 2 diabetes (T2D) is a progressive metabolic disorder characterised by obesity, insulin resistance, impaired glucose tolerance, and hyperglycaemia. The long time-course of T2D in humans makes accurate modelling of sustained T2D in animal models difficult. The goal of this study was to develop and characterise an accurate and reproducible, non-transgenic model of sustained T2D in mice. Adult, male C57BL/6 mice were placed on a high-fat diet (HFD) for 17 weeks. From weeks 3–5, osmotic mini-pumps were implanted subcutaneously to slowly infuse streptozotocin (STZ; 200–350 mg/kg) for 14-days after which mini-pumps were removed. Body weight, blood glucose concentration, and glucose tolerance were monitored for 12 weeks post STZ treatment. Our data demonstrate that the combination of HFD and 200 mg/kg STZ delivered by mini-pump leads to increased blood glucose concentrations and impaired glucose tolerance, while maintaining obesity and hepatic dyslipidaemia. In week 17, plasma insulin concentration was assessed and showed that with STZ treatment, mice still produce insulin, but that this is reduced compared with mice on HFD only. Lastly, we examined pancreas sections using immunohistochemistry and show that there is no overt loss of beta cell mass. In conclusion, we demonstrate development of a reproducible in vivo model of T2D in mice that replicates a number of key pathophysiological changes seen in humans with T2D.

Keywords High fat diet, Streptozotocin, Type 2 diabetes, Obesity, Insulin resistance, Mouse model

Type 2 diabetes (T2D) is a complex and progressive metabolic disorder that affects approximately 380 million people globally[1]. The greatest risk factor for developing T2D is being overweight or obese, and due to the increasing prevalence of obesity, the number of people with T2D is predicted to rise to 642 million by 2040[2,3]. These estimates are likely to be conservative, as the proportion of overweight or obese people with undiagnosed insulin resistance and/or T2D is proposed to be as high as 50%[4]. As such, many people may unknowingly be living with insulin resistance and mild to moderate hyperglycaemia, the primary risk factor for development of T2D complications such as neuropathy, nephropathy, retinopathy and cardiovascular disease[2,3,5–7]. Despite this, we do not fully understand the mechanisms that drive development of T2D or subsequent development of comorbid complications, partly due to limitations of accurate and reproducible animal models currently available. Therefore, development of animal models that more closely resemble human T2D is a critical step in expanding our understanding of T2D pathophysiology and designing new preventative and therapeutic strategies to combat the increasing prevalence and impact of this disease.

One challenge of modelling T2D in animals, particularly in rodents, is that the time course of T2D progression in humans is often long (10–15 years). The cumulative nature of obesity-associated insulin resistance and T2D means humans typically progress through several distinct stages. In obesity-associated insulin resistance, the earliest metabolic changes noted are a decrease in peripheral insulin sensitivity[5,7] followed by compensatory hyperinsulinaemia as pancreatic beta cells are stimulated to produce more insulin in an attempt to maintain normal blood glucose concentrations[5,7,8]. Over time, the increased demand for insulin culminates in pancreatic beta cell failure resulting in insufficient insulin production and subsequent hyperglycaemia characteristic of established T2D[5]. Although rodent models exist that can replicate obesity and insulin resistance using dietary modifications, without further intervention, these animals do not progress to T2D[9,10]. For this reason,

Tasmanian School of Medicine, College of Health and Medicine, University of Tasmania, Hobart, TAS 7000, Australia. ✉email: Dino.Premilovac@utas.edu.au

streptozotocin (STZ), a DNA alkylating agent that enters pancreatic beta cells via the GLUT2 transporter, has been utilised in numerous studies[10–15] to deplete beta cells, resulting in subsequent hyperglycaemia.

Over the past 50 years, STZ has generally been administered intraperitoneally as either a single high dose injection or multiple low dose injections[13]. Single high dose STZ injections typically leads to complete beta cells death causing rapid and severe hyperglycaemia, which does not reflect the much slower progression of human T2D[16–20]. Multiple low dose STZ injections can impair beta cell function leading to transient hyperglycaemia which similarly fails to reproduce progression of human T2D over time[21–24]. To overcome this, our group has recently optimised the use of osmotic mini-pumps in rats to slowly infuse STZ at a low constant rate across 14 days[25,26]. Delivering STZ using this method leads to moderate and sustained hyperglycaemia for at least 15 weeks while maintaining obesity. This rat model has provided a useful platform to investigate the development of T2D co-morbidities, namely retinopathy and neuropathy[26,27]. The primary aim of the current study is to establish a reproducible mouse model to enable targeted and sustained induction of different stages of T2D. This new approach provides an opportunity to broaden the potential for mechanistic insight to understand the development of insulin resistance and T2D, in addition to co-morbidities associated with T2D.

Methods

Animal husbandry

All experimental procedures were approved by the University of Tasmania Ethics Committee (A0018283) and performed in accordance with the Australian Code for the Care and Use of Animals for Scientific Purposes – 2013, 8th Edition and adhered to the ARRIVE guidelines. Male *Tg(Cspg4-DsRed.T1)1Akik/J* (Jackson Laboratories, USA; #008,241) mice backcrossed onto a C57BL/6 background were used for all experiments. This transgenic mouse line was utilised to enable microvascular analysis (common T2D pathology) to be performed in future experiments without the need for additional animals. At 11 weeks of age, mice were acclimatised for seven days prior to random allocation to specific experimental conditions. Mice were housed in standard conditions at 21 ± 2 °C with a 12h–12h light–dark cycle for the duration of the experiment. Animals were provided with water and chow ad libitum throughout the study. With the exception of control diet (CD; 6% fat wt/wt; n = 5) fed mice, all other groups were provided with a high fat diet (HFD; 23% fat wt/wt; Specialty Feeds, Australia; #SF15-059).

STZ preparation and osmotic mini-pump implant

Previous experiments using STZ delivered via osmotic mini-pumps were performed in rats[25–27]. Therefore, a series of preliminary experiments were conducted in mice to establish the dose response relationship of STZ using the osmotic mini-pump method (see supplementary material). From this work, we chose to undertake long-term evaluation of > 250mg/kg (HFD + highSTZ; n = 7) STZ as this group exhibited mild hyperglycaemia and glucose intolerance within the two week STZ delivery period (Supplementary Fig. 1). In addition, the 200mg/kg (HFD + lowSTZ; n = 5) group was also monitored long term to assess whether hyperglycaemia and glucose intolerance developed over time (Supplementary Fig. 1). Following three weeks of HFD, STZ (Sigma Aldrich, USA) was prepared in citrate buffered saline (0.1mmol/L; pH 4.4) and a total volume of 100µL was loaded into each osmotic mini-pump (Alzet Model 1002; Durect Corporation, USA) immediately prior to subcutaneous implantation. The method for pump implantation was adapted from Premilovac et al. (2017) and is thoroughly described in Attrill et al. (2023)[25,28]. Briefly, mice were anaesthetised (isoflurane, 5% induction, 2–3% maintenance) and received a subcutaneous injection of meloxicam (5mg/kg, Ilium, Australia). Mini-pumps containing STZ were implanted subcutaneously on the animal's dorsum, and then removed after 14-days. Mice in the sham group (HFD + SHAM; n = 5) received the same surgical procedures but did not have a mini-pump implanted.

Assessment of metabolic alterations

Body weight and non-fasting blood glucose concentrations were assessed weekly at a consistent time of day (1 pm; see Fig. 1). Blood glucose concentrations were determined using a hand-held glucometer (Accu-Chek Performa; Roche Diagnostics, Australia) and a blood sample was collected by tail tip incision. To assess changes in glucose tolerance, each animal underwent a glucose tolerance test (GTT) at week 5 (immediately following 14 days of STZ delivery). To do this, animals were fasted for 6 h and then received an intraperitoneal injection of glucose (2 g/kg). Blood glucose concentration was then assessed repeatedly across 2 h. Due to limitations of the glucometer (maximal glucose concentration measurement of 33.3 mmol/L), fasting blood glucose (0 min) and the final glucose measurement (2 h post glucose injection) were used to compare the metabolic defects between groups. GTT were repeated in weeks 9, 13 and 17 to track changes in glucose tolerance after osmotic mini-pump (and hence STZ) removal. At the conclusion of the 17 week protocol, arterial blood was collected using cardiac puncture and plasma TNFα (Mouse TNFα ELISA kit; ELISAKIT.com; Australia) and insulin (Insulin ELISA; Mercodia, Sweden) concentrations was determined using an ELISA according to manufacturer's instructions.

Adipocyte, liver and pancreas histology

At the conclusion of week 17, all mice were injected intraperitoneally with a lethal dose of pentobarbitone (200 mg/kg). After confirmation of deep anaesthesia, animals were transcardially perfused with phosphate buffered saline (PBS), followed by 4% paraformaldehyde (PFA; pH 7.4). Epididymal fat pads were dissected and weighed to assess adiposity between the groups. The epididymal fat pad, liver and pancreas were post fixed in 4% PFA for 1.5 h.

Epididymal fat pads were paraffin embedded using the Leica ASP200 Autoprocessor (Leica Biosystems, Germany) which completed the following steps: 1 h in 70% ethanol, 1 h in 90% ethanol, 1.5 h in 100% ethanol (×4), 1 h in xylene (×2) and 1 h in paraffin wax (×3). Epididymal fat pads were sectioned at 7µm thick on a microtome (Leica RM225; Leica Biosystems, Germany) and mounted onto IHC Flex microscope slides (Dako,

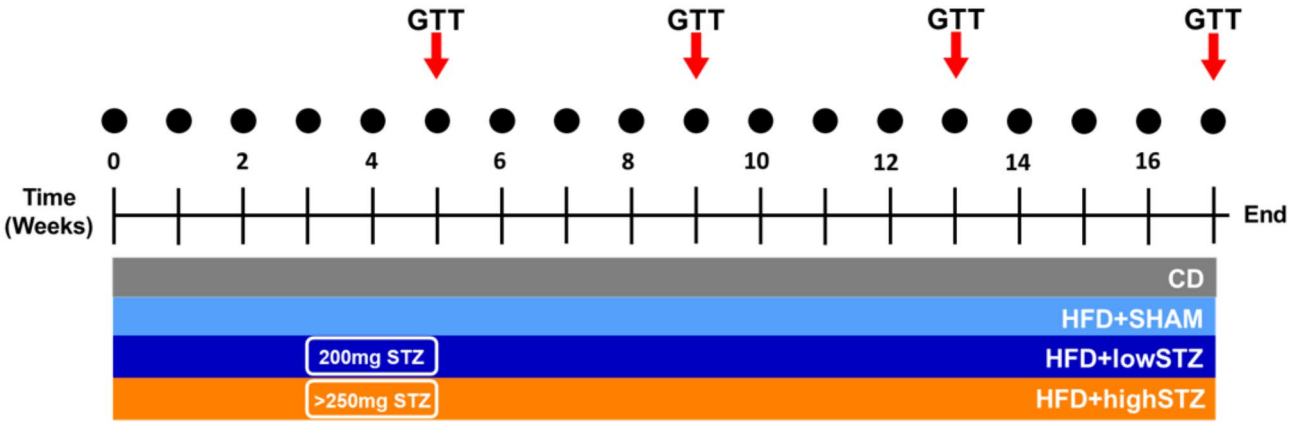

Fig. 1. Experimental timeline All mice underwent a 17-week intervention and were provided either control (6% fat w/w, n = 5) or a HFD (23% fat w/w) ad libitum. Mice on the HFD had osmotic mini-pumps implanted subcutaneously from weeks 3–5 to deliver 200 mg/kg STZ (HFD + lowSTZ, n = 5) or greater than 250 mg/kg STZ (HFD + highSTZ, n = 7). Animals in the HFD + SHAM group (n = 5) had the surgical procedures but did not have a mini-pump implanted. Body weight and non-fasting blood glucose were assessed weekly. Glucose tolerance tests (GTT; 2 g/kg body weight) were performed in weeks 5, 9, 13 and 17. All animals were euthanised in week 17 to collect plasma, adipose, liver and pancreas tissue samples for analysis.

Denmark) for standard H&E staining (see Parlee et al.[29]). Slides were imaged at 20× magnification on an Olympus VS200 Virtual Slide System (Olympus, Japan) and adipocyte size was determined using QuPath 0.5.1 (method detailed in Palomāki et al.[30]). Approximately 300 adipocytes were measured for each animal to generate average adipocyte size.

Liver and pancreas samples were cryoprotected in 30% sucrose solution overnight at 4 °C prior to embedding in optimal cutting temperature compound (OCT; Agilent Technologies, USA). Frozen samples were then sectioned (Leica CM-1850; Leica Biosystems, Germany) at − 23 °C and immediately mounted onto IHC Flex microscope slides (Dako, Denmark).

Liver samples were cut at 10µm thick and stained with oil red O (ORO; method detailed in Mehlem et al.[31]). Briefly, ORO was mixed in isopropyl alcohol (6.25 g/L) to form a stock solution that was diluted with water (1.5 parts stock solution to 1 part water) and filtered (0.22 µm filter) immediately prior to use. Liver sections were incubated in ORO for 5 min, followed by thorough washing in running water. Coverslips were placed using fluorescence mounting medium (Dako, Denmark) and slides were immediately imaged at 20× magnification on an Olympus VS200 Virtual Slide System (Olympus, Japan). Three, 1 mm^2 regions were analysed using ImageJ (version 1.52i; NIH, USA) following the protocol detailed in[31] to assess lipid area.

Pancreas samples were cut at 20 µm thickness and incubated overnight at 4 °C in PBS containing 4% donkey serum, 0.4% triton-X-100 and pan-insulin antibody (insulin and pro-insulin; 1:500; Abcam, UK; #ab8304). Sections were washed with PBS and then incubated in the dark for 1h at room temperature in PBS containing 4',6-diamidino-2-phenylindole (DAPI; 1:20,000; Sigma Aldrich, USA) and Alexa-Fluor conjugated secondary antibody donkey anti-mouse 647 (1:1000; Life Technologies Australia, Australia; #A21236). Sections were washed in PBS and glass coverslips were mounted using fluorescence mounting medium (Dako, Denmark). To assess changes in proliferation within Islets of Langerhans, a second series of pancreas sections was probed with rabbit anti-Ki67 antibody (1:1000; Abcam; #ab15580) following the same protocol as above for pan-insulin staining. To assess changes in apoptosis within Islets of Langerhans, terminal deoxynucleotidyl transferase dUTP nick end labelling (TUNEL) staining was performed on a separate set of sections as per the manufacturers instructions (Click-iT™ Plus TUNEL Assay Kits for In Situ Apoptosis Detection; ThermoFischer Scientific; #C10619). Following the TUNEL protocol, all slides were subsequently probed with pan-insulin and DAPI as per the protocol above. All slides were stored in the dark at 4 °C until required for imaging. Slides were imaged at 20× magnification using extended focal imaging on an Olympus VS120 Virtual Slide System (DAPI:388 nm, 50 ms; Insulin/pro-insulin: 647 or 488 nm, 200 ms; Ki67: 647, 200 ms; TUNEL:647, 300 ms; Olympus, Japan) and analysed using ImageJ (version 1.52i; NIH, USA). Pancreatic islets were identified using DAPI staining, and area of pan-insulin staining was calculated as a percentage of total pancreatic islet area. For quantification of proliferation and apoptosis, Ki67 or TUNEL positive cells within the pancreatic islets were manually counted and the percentage of all islet cells expressing each marker was calculated as published by others.

Data and statistics

Statistical and graphical analysis was performed using GraphPad Prism 10 (GraphPad, USA). Metabolic data across time was assessed using two-way repeated measures ANOVA with Tukeys post hoc test. Single time-point and immunohistochemical data were assessed using a one-way ANOVA with Tukeys post hoc test. All data presented as mean and standard deviation. A p-value < 0.05 was considered statistically significant.

Results

Body weight and adiposity

Body weight was measured weekly throughout the experiment (Fig. 2a). All groups of mice gained weight across the 17-week protocol ($p < 0.001$). Prior to STZ treatment in week 3, all HFD-fed mice had gained significantly more body weight compared to CD-fed mice (2.2 ± 1.5 vs. 5.2 ± 1.8g, $p = 0.003$). In week 5, compared to CD there was no difference in body weight gained in the HFD + SHAM ($p = 0.140$), HFD + lowSTZ ($p = 0.245$) or the HFD + highSTZ ($p = 0.882$) groups. However, by week 17 mice in both the HFD + SHAM (7.4 ± 2.7 vs. 14.2 ± 3.6g, $p = 0.044$) and the HFD + lowSTZ (7.4 ± 2.7 vs. 15.2 ± 2.0g, $p = 0.005$) groups had gained approximately twofold more body weight compared to CD.

After mice were euthanised in week 17, epididymal fat pads were excised and weighed as a surrogate marker for adiposity (Fig. 2b). Compared to CD, epididymal fat mass was approximately twofold higher in the HFD + SHAM group (1.3 ± 0.5 vs. 2.7 ± 0.3g, $p = 0.017$). However, there was no change in epididymal fat mass in the HFD + lowSTZ ($p = 0.066$) or HFD + highSTZ ($p = 0.420$) groups compared to CD. In addition to epididymal fat mass, adipocyte area was also assessed (Fig. 2c and d). Both the HFD + SHAM group (3524 ± 1400 vs. 8227 ± 1053 μm^2, $p < 0.001$) and the HFD + lowSTZ group (3524 ± 1400 vs. 6713 ± 1746 μm^2, $p = 0.007$) had elevated adipocyte area compared to the CD group and this effect was lost with high dose STZ (3524 ± 1400 vs. 4610 ± 1432 μm^2, $p = 0.438$).

To assess pathological lipid accumulation, lipid load in the liver was assessed by ORO staining (Fig. 2c and e). Compared to the CD group, the HFD + SHAM (1.5 ± 1.1 vs. 15.1 ± 8.1%, $p = 0.017$), the HFD + lowSTZ (1.5 ± 1.1 vs. 19.8 ± 5.2%, $p = 0.002$) and the HFD + highSTZ (1.5 ± 1.1 vs. 18.9 ± 7.9%, $p = 0.001$) groups each had elevated liver lipid accumulation.

Non-fasting blood glucose, plasma insulin and TNFα concentration

Non-fasting blood glucose concentration was assessed weekly throughout the experiment (Fig. 3a). Prior to mini-pump implants, there was no difference in non-fasting glucose between CD and HFD fed groups ($p = 0.160$). Similarly, immediately post STZ treatment (week 5), there were no differences in non-fasting blood glucose between any groups ($p = 0.371$). Whilst in week 17, there was no difference in non-fasting blood glucose in both the HFD + SHAM ($p = 0.362$) and the HFD + lowSTZ ($p = 0.998$) groups compared to CD, non-fasting blood glucose concentration was approximately twofold higher in the HFD + highSTZ group (8.4 ± 0.9 vs. 16.8 ± 6.6 mmol/L, $p = 0.016$). Non-fasting blood glucose in the HFD + highSTZ group was also elevated compared to both the HFD + SHAM (9.4 ± 1.3 vs. 16.8 ± 6.6mmol/L, $p = 0.030$) and HFD + lowSTZ (9.1 ± 0.8 vs. 16.8 ± 6.6 mmol/L, $p = 0.016$) groups.

After identifying changes in blood glucose concentration, non-fasting plasma insulin concentration was assessed in week 17 when a larger quantity of arterial blood could be collected via cardiac puncture (Fig. 3b). Compared to the CD group, plasma insulin concentration was increased in the HFD + SHAM mice (165 ± 18 vs. 242 ± 109 pmol/L, $p = 0.003$) following 17 weeks of HFD feeding. Treatment with either low ($p < 0.001$) or high-dose ($p < 0.001$) STZ attenuated this effect, reducing plasma insulin concentration compared to the HFD + SHAM group, seemingly back to CD levels (HFD + lowSTZ $p = 0.109$; HFD + highSTZ $p = 0.431$).

Finally, we assessed systemic inflammation by measuring plasma TNFα concentrations at the end of the intervention (Fig. 3c). Compared to the CD group, mice in the HFD + SHAM group had a twofold increase in circulating TNFα concentrations (3.69 ± 0.92 vs. 7.79 ± 1.46 pg/mL, $p = 0.006$). While mice in the HFD + lowSTZ group had increased circulating TNFα concentrations compared with CD (3.69 ± 0.92 vs. 9.02 ± 0.95 pg/mL, $p < 0.001$), these were not different compared to HFD + SHAM (7.79 ± 1.46 vs. 9.02 ± 0.95 pg/mL, $p = 0.615$). In contrast, mice in the HFD + highSTZ group had markedly increased circulating TNFα concentrations compared to both CD (3.69 ± 0.92 vs. 10.82 ± 2.15 pg/mL, $p < 0.001$) and HFD + SHAM (7.79 ± 1.46 vs. 10.82 ± 2.15 pg/mL, $p = 0.021$). There was no difference in circulating TNFα concentrations between the HFD + lowSTZ and HFD + highSTZ groups (9.02 ± 0.95 vs. 10.82 ± 2.15 pg/mL, $p = 0.247$).

Islet of Langerhans morphology and cellular turnover.

After identifying changes in blood glucose and plasma insulin concentration, the integrity of pancreatic Islets of Langerhans was assessed by a range of measures (Fig. 4a–e). There were no differences in islet density, islet area, islet cell density or proinsulin/insulin staining between any groups. Similarly, assessment of cell proliferation (Supplementary Fig. 2) and apoptosis (Supplementary Fig. 3) within Islets of Langerhans revealed no major differences between any of the groups.

Fasting blood glucose

Fasting blood glucose concentration was measured following a 6h fast as part of the GTT in weeks 5, 9, 13 and 17 (Fig. 5a). In week 5, there was no difference in fasting blood glucose in the HFD + SHAM ($p = 0.113$) group compared to CD however, treatment with STZ increased fasting blood glucose in both the HFD + lowSTZ (9.0 ± 1.6 vs. 12.6 ± 1.4mmol/L, $p = 0.023$) and HFD + highSTZ (9.0 ± 1.6 vs. 15.9 ± 4.9mmol/L, $p = 0.035$). Despite this, there was no difference in fasting blood glucose in the HFD + SHAM group compared to both the HFD + lowSTZ ($p = 0.979$) and the HFD + highSTZ ($p = 0.340$) groups.

A similar pattern persisted until week 17 with no difference in fasting blood glucose between the CD and HFD + SHAM ($p = 0.233$) groups and elevated fasting blood glucose in both the HFD + lowSTZ (9.4 ± 1.0 vs. 13.3 ± 1.4 mmol/L, $p = 0.010$) and HFD + highSTZ (9.4 ± 1.0 vs. 19.8 ± 5.4 mmol/L, $p = 0.014$) groups compared to CD. In addition, by week 17 the HFD + highSTZ group had elevated fasting blood glucose concentration compared to the HFD + SHAM group (10.9 ± 0.4 vs. 19.8 ± 5.4 mmol/L, $p = 0.026$).

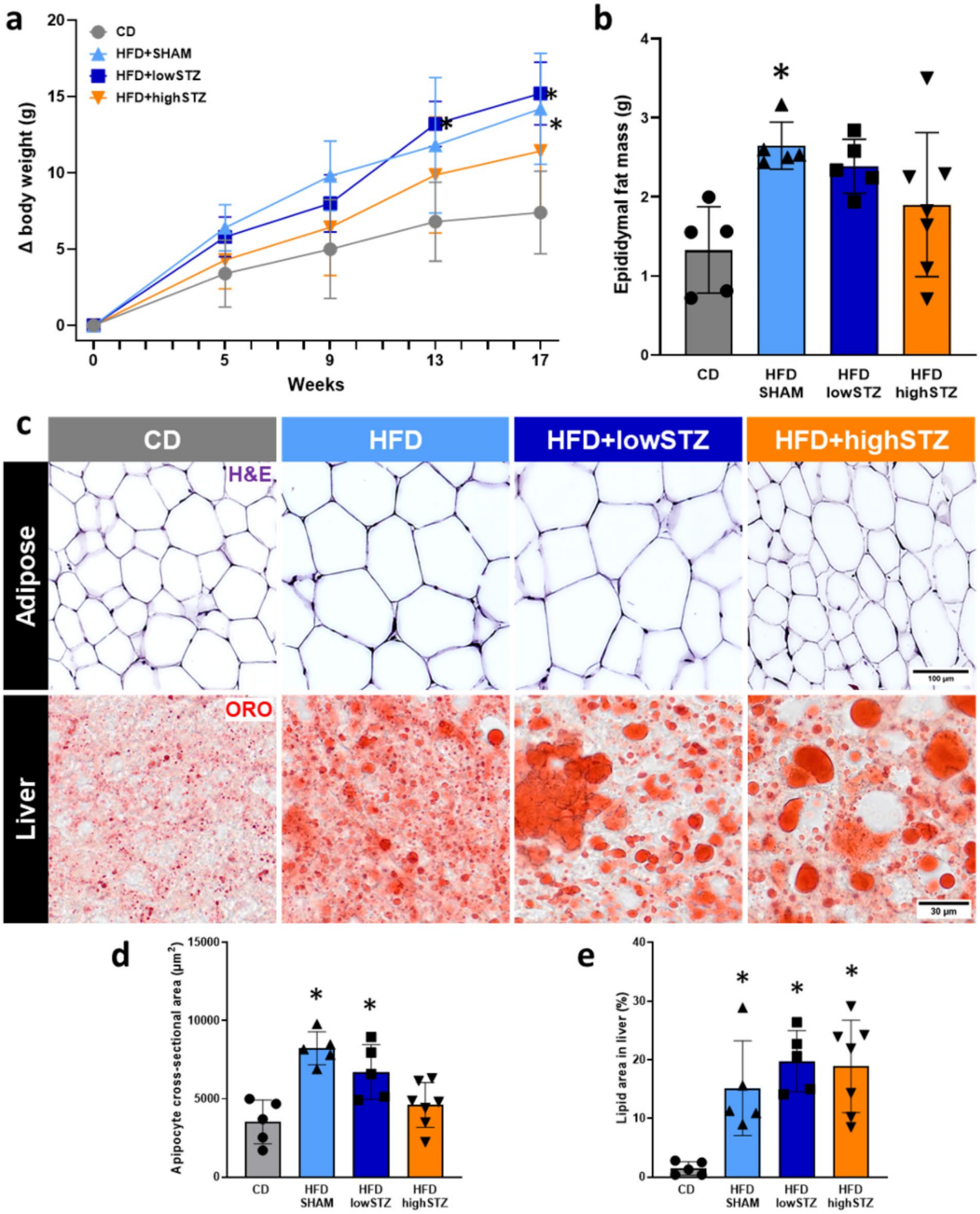

Fig. 2. Combination of HFD and STZ delivered by osmotic mini-pump increases body weight and adiposity which is sustained over time. (**A**) Average change in body weight over the 17 week treatment period. (**B**) Week 17 epididymal fat pad weight. (**C**) Representative images of epididymal fat pad adipocytes stained with H&E (upper panels) and liver samples stained with oil red O (ORO; lower panels). (**D**) Average adipocyte cross-sectional area. (**E**) Lipid area in the liver. Data are mean ± SD for n = 5–7. Two-way repeated measure ANOVA with Tukeys post hoc test was used to analyse data in panel (**A**). One-way ANOVA with Tukeys post hoc test was used to analyse data in panel (**B**), (**D**) and (**E**). *$p < 0.05$ compared to CD.

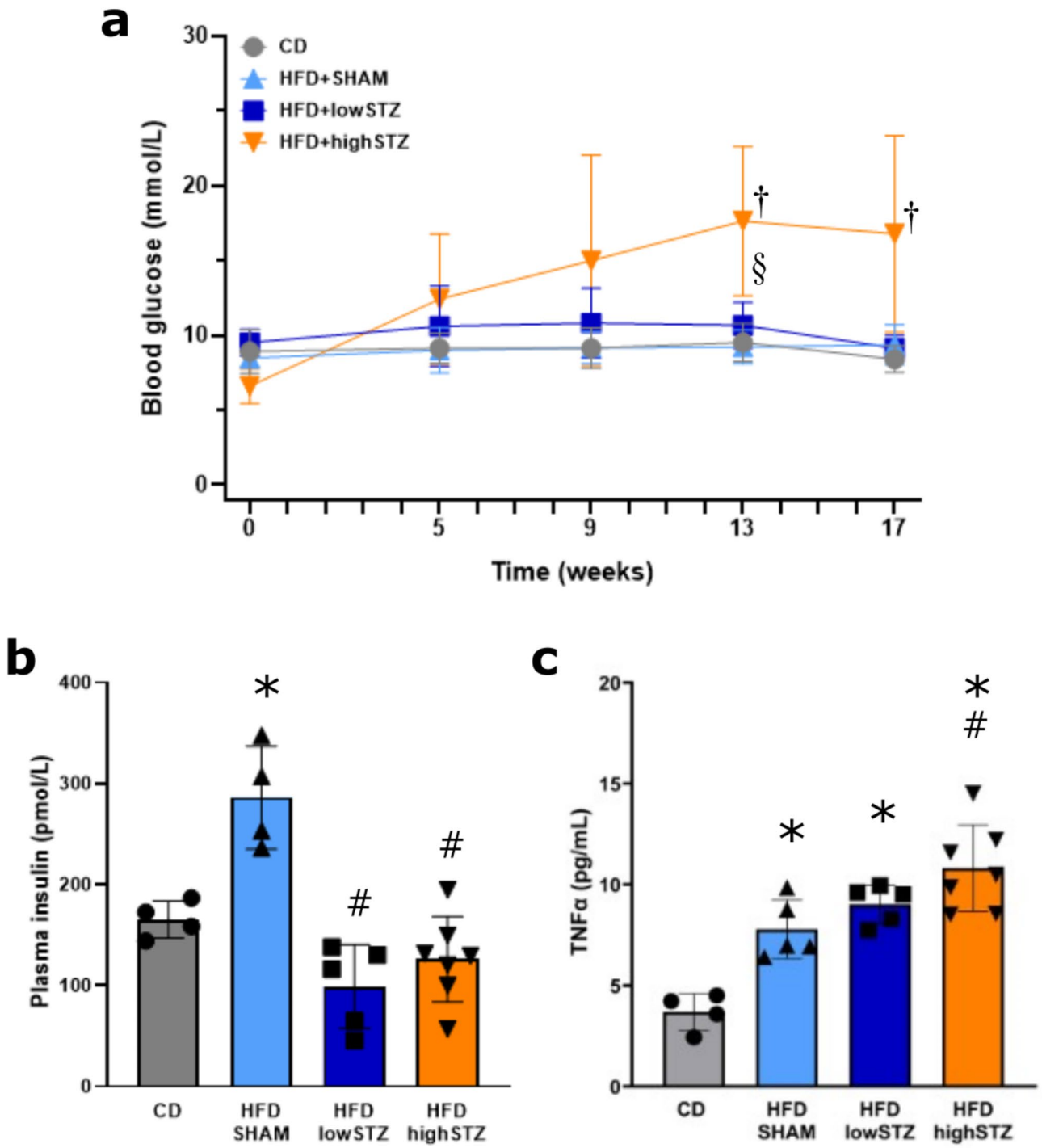

Fig. 3. The combination of HFD and high-dose STZ delivered by osmotic mini-pump increases non-fasting blood glucose and TNFα without reducing plasma insulin concentration. (**A**) Non-fasting blood glucose level over 17-week intervention. (**B**) Non-fasting plasma insulin concentration in week 17. (**C**) Plasma TNFα concentration in week 17. Data are mean ± SD for n = 5–7. Two-way repeated measure ANOVA with Tukeys post hoc test was used to analyse data in (**A**) and a one-way ANOVA with Tukeys post hoc test was used to analyse data in (**B**). *$p < 0.05$ compared to CD at same timepoint. #$p < 0.05$ compared to HFD + SHAM at same timepoint. †$p < 0.05$ compared to all other groups at the same timepoint. §$p < 0.05$ compared to week 0 within group.

Glucose tolerance

Glucose tolerance was assessed in weeks 5, 9, 13 and 17 (Fig. 5b) by sampling blood glucose concentration 2h-post intraperitoneal injection of 2 g/kg glucose. In week 5, there was no difference in 2h blood glucose in the HFD + SHAM ($p = 0.490$) and HFD + lowSTZ ($p = 0.370$) groups compared to CD. In contrast, 2 h blood

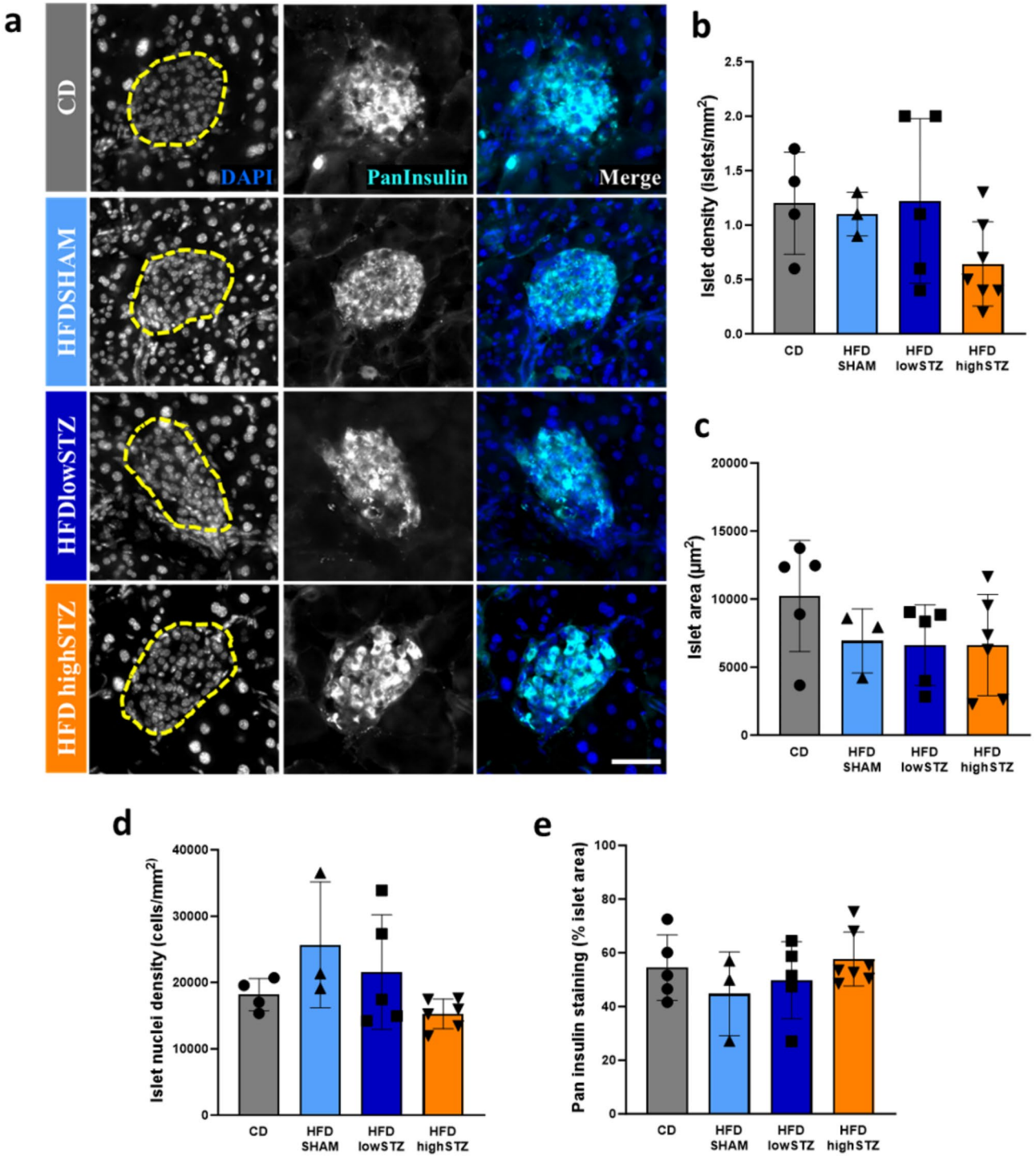

Fig. 4. Combination of HFD and STZ does not alter pancreatic islet morphology. Pancreas histology was performed in week 17 to assess the extent of pancreatic beta cell depletion in response to STZ. (**A**) Pancreatic sections were assessed for pan-insulin (cyan; labels proinsulin and insulin) and counter stained with DAPI to visualise nuclei, allowing identification of islets of Langerhans (dashed line). (**B**) Number of islets per mm^2 of pancreas across the treatment groups. (**C**) Average islet area. (**D**) Average number of nuclei per mm^2 of islet. (**E**) Percent of islet area with positive pan-insulin immunoreactivity. Data are mean ± SD for n = 3–7. Scale bar = 50 µm. One-way ANOVA with Tukeys post hoc test was used to analyse data. $^*p < 0.05$ compared to CD. $\#p < 0.05$ compared to HFD + SHAM.

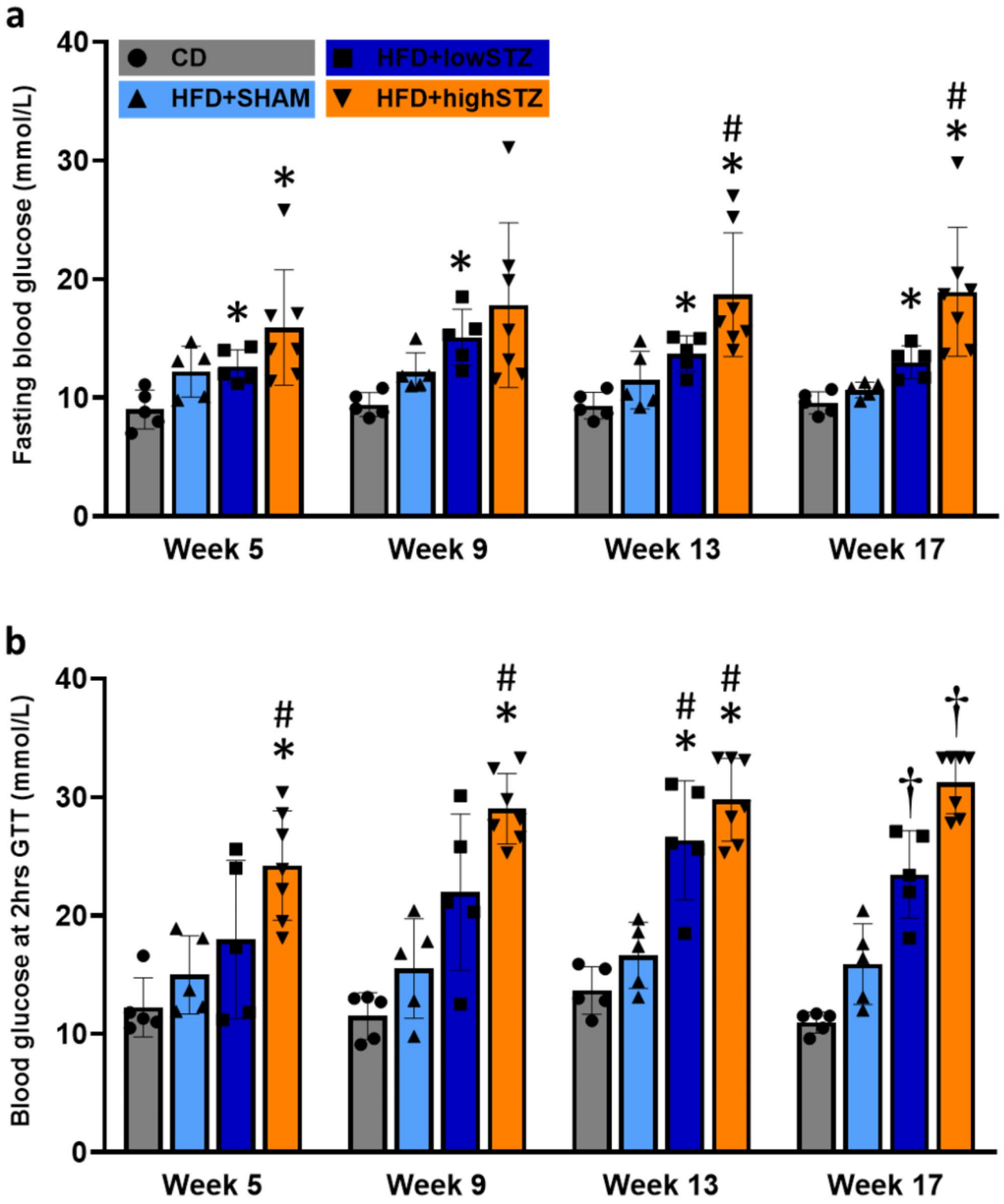

Fig. 5. Combination of HFD and low-dose STZ increases fasting blood glucose and worsens glucose intolerance across 17 weeks. Glucose tolerance tests (GTT; 2 g/kg) were performed in week 5, 9, 13, and 17 to assess fasting blood glucose concentration and glucose tolerance. (**A**) Fasting blood glucose immediately prior to GTT. (**B**) Blood glucose concentration 2h after injection of glucose. Data are mean ± SD for n = 5–7. Two-way repeated measure ANOVA with Tukeys post hoc test was used to analyse data. *$p < 0.05$ compared to CD at the same timepoint. #$p < 0.05$ compared to HFD + SHAM at the same timepoint. †$p < 0.05$ compared to all other groups at the same timepoint.

glucose concentration was elevated in the HFD + highSTZ group compared to both the CD (12.2 ± 2.5 vs. 24.2 ± 4.6mmol/L, $p = 0.001$) and HFD + SHAM (15.0 ± 3.3 vs. 24.2 ± 4.6mmol/L, $p = 0.011$) groups in week 5.

By week 17, a dose-dependent increase in 2h blood glucose concentration was noted, indicative of a dose-dependent decline in glucose tolerance. Whilst there was no difference in 2h blood glucose between the HFD + SHAM ($p = 0.097$) compared to CD, by week 17 (12 weeks post STZ) 2h blood glucose was approximately twofold higher in the HFD + lowSTZ group (10.8 ± 0.9 vs. 24.8 ± 2.5mmol/L, $p = 0.004$) and approximately threefold higher in the HFD + highSTZ group (10.8 ± 0.9 vs. 30.9 ± 2.7mmol/L, $p < 0.001$). In addition, both the HFD + lowSTZ (15.8 ± 3.9 vs. 24.8 ± 2.5mmol/L, $p = 0.040$) and HFD + highSTZ (15.8 ± 3.9 vs. 30.9 ± 2.7mmol/L, $p < 0.001$) groups had markedly elevated 2h blood glucose compared to the HFD + SHAM group however, this was more pronounced in the high-dose group compared to low-dose (24.8 ± 2.5 vs. 30.9 ± 2.7mmol/L, $p = 0.021$).

Discussion

In the present study, we demonstrate development of a novel model for accelerated and sustained induction of T2D in mice by combining high fat diet feeding with STZ delivered by osmotic mini-pump. In our model, HFD feeding led to increased adiposity and plasma insulin concentration, reflecting obesity and insulin resistance characteristic of human disease[5,7,32]. Importantly, this obese, insulin resistant phenotype was maintained with the addition of low dose STZ (200mg/kg) delivered by osmotic mini-pump. We show that treatment with STZ increased circulating blood glucose concentrations and decreased glucose tolerance in a dose dependent manner. Importantly, these metabolic changes were sustained 12 weeks after removal of mini-pumps containing STZ indicating a long-lasting shift in glucose homeostasis. In addition, both the lower and higher doses of STZ reduced plasma insulin concentrations to control levels without overtly impacting pancreatic islet morphology. These data indicate that osmotic mini-pump delivered STZ induces long-term pancreatic beta cell dysfunction rather than beta cell death to limit, but not completely remove insulin production. Therefore, we show that using HFD and low dose STZ (200 mg/kg) delivered by osmotic mini-pump generates a mouse model that displays four key human T2D characteristics simultaneously (obesity, insulin resistance, hyperglycaemia, systemic inflammation and glucose intolerance) that are sustained for the 17 week time course used in this experiment. This new approach overcomes critical limitations previously experienced with STZ models of T2D and provides a useful tool for investigating the progression of T2D and commonly associated co-morbidities.

Once in circulation, STZ enters cells using the GLUT-2 transporter[33,34]. Whilst present in several tissues such as liver and gut epithelium[35], the GLUT-2 transporter is abundant on the surface of pancreatic beta cells making them particularly susceptible to STZ's intracellular effects. In beta cells, STZ interferes with cellular processes that culminate in DNA damage and cell death[33,34], ultimately reducing beta cell number and therefore the insulin producing capability of the pancreas[33]. Numerous studies have utilised the combination of HFD-feeding and STZ injections to impair glucose tolerance in rodents[13,25–27] however, the resulting shift in metabolic homeostasis can vary greatly depending on the animal strain, dose of STZ and the number of injections used[22]. Recent work by our research group has endeavoured to improve the efficacy of the model by slow infusion of STZ using osmotic mini-pumps. Our work has demonstrated that the combination of HFD and osmotic mini-pump delivered STZ can be used to control induction of different stages of T2D in different strains of rats that is sustained for at least 3 months[25–27]. In the current study, we demonstrate that the application of this methodology can cause similarly consistent and sustained induction of T2D in C57BL/6 mice.

Historically, STZ has been delivered by injection into the peritoneal, subcutaneous or vascular space[22,36]. This method of delivery generates variable results due to rapid peaks and troughs in circulating STZ concentration and therefore beta cell damage/depletion. When mice are injected with lower doses (40–75mg/kg), STZ causes temporary hyperglycaemia, therefore requiring repeat injections to maintain a hyperglycaemic phenotype for longer time-periods[36,37]. The cumulative effect of repeat injections of STZ (which has effects beyond beta cells) therefore makes it difficult to determine impact of T2D or repeat STZ in such experiments. In contrast, mice injected with higher STZ doses (> 150 mg/kg) exhibit severe hyperglycaemia likely due complete beta cell death and loss of insulin production[6,38]. These mice are therefore susceptible to drastic weight loss and there is generally a higher mortality rate in these experiments[18–20]. Until recently, immediate injection of STZ was considered the only viable method of delivery, as STZ was proposed to degrade quickly once in solution; a dogma that is changing since anomer equilibrated STZ may be more reliable for inducing disease[25,39,40]. Previous work using HFD feeding and delivery of STZ via osmotic mini-pump in rats[25–27] and current work in mice suggests that low, but consistent, circulating STZ imparts more control over the resulting metabolic phenotype. We have previously shown that once dissolved in citrate buffered saline, STZ reaches anomer equilibration within ~ 120 min and remains relatively stable for 14 days. For this reason, the slow infusion of the anomer equilibrated STZ using the osmotic mini-pump method may explain the improved reproducibility between this method and injection methods. It is important to note that the mortality rate in the current study was zero, while some studies utilising injectable STZ report mortality rates of as much as 20–30% within 30 days of administration[18,41]. The reproducibility of the resulting phenotype and reduced mortality/animal welfare impact using this methodology strongly aligns with the NC3R's recommendations and guidelines[42]. From an animal welfare perspective alone, this is a major advance in the field.

Beyond dietary and pharmacological models, previous studies have relied heavily on genetic models of T2D, with the most popular being the *ob/ob* (leptin deficient) and *db/db* (leptin receptor deficient) mouse strains. These genetic models develop some of the key T2D traits and have been a mainstay of T2D research for decades[43]. However, these mouse strains have problems with normal leptin signalling contributing to developmental changes and subsequent compensation across several systems (eg. beta cell hyperplasia, transient hyperglycaemia normalised by 5 months)[43–45]. In addition, there are increasing reports of the non-metabolic roles of leptin, indicating leptin signalling deletion in mice likely impacts multiple systems and has effects beyond metabolism alone[46,47]. In addition, many genetic mouse models of T2D are considered sub-fertile making them difficult to

breed with other strains of interest[48–50]. In the present study, we adapted the use of HFD and STZ delivered by osmotic mini-pump to reliably induce T2D in adult C57BL/6 mice – one of the most common mouse strains used in research. Importantly, adapting our method for use in mice provides a platform for induction of T2D in any number of mouse strains with transgenic manipulations to identify specific mechanisms that contribute to development/progression of T2D and the related co-morbidities.

Whilst the combination of HFD and STZ delivered by osmotic mini-pump in mice provides an important tool, there remain limitations regarding this model. The methodology we have utilised remains artificial for induction of T2D in mice and therefore differs from the natural, long-term human T2D pathogenesis. Human T2D progresses through several stages including obesity associated insulin resistance and hyperinsulinemia which over time culminate in beta cell dysfunction and consequently death[5,7]. Whilst our mouse model involves HFD-induced insulin resistance[8,51–54], pancreatic beta cell depletion with STZ does not replicate the cause of beta cell death seen in human T2D. Despite this, the benefit of using STZ is that it accelerates development of hyperglycaemia which may not otherwise occur using a HFD within the short rodent lifespan. Importantly, the result of human T2D and HFD-feeding with STZ treatment in mice are similar, concurrent obesity and hyperglycaemia which drive development of the major pathological features of T2D. Another important limitation of this study is that we have only used male mice in our experiments. Whether female mice would similarly respond to the current methodology is not known and needs to be determined in future studies with the current study providing a platform to undertake this work.

In conclusion, the current study demonstrates a novel method for inducing T2D in mice that enables targeted and sustained induction of different stages of T2D while maintaining a state of obesity. This model in combination with the large number of transgenic mouse strains provides a powerful platform for investigating mechanisms of T2D, associated pathologies and importantly identifying potential therapeutic strategies.

Data availability

All data collected for this study is available in the manuscript. The data generated is available from the corresponding author for any interested party on reasonable request.

Received: 10 July 2024; Accepted: 3 February 2025
Published online: 14 March 2025

References

1. Roglic, G. WHO Global report on diabetes: A summary. *Int. J. Noncommun. Dis.* **1**, 3–8 (2016).
2. Ogurtsova, K. et al. IDF Diabetes Atlas: Global estimates for the prevalence of diabetes for 2015 and 2040. *Diabetes Res. Clin. Pract.* **128**, 40–50. https://doi.org/10.1016/j.diabres.2017.03.024 (2017).
3. Chen, L., Magliano, D. J. & Zimmet, P. Z. The worldwide epidemiology of type 2 diabetes mellitus–present and future perspectives. *Nat. Rev. Endocrinol.* **8**, 228–236. https://doi.org/10.1038/nrendo.2011.183 (2011).
4. Beagley, J., Guariguata, L., Weil, C. & Motala, A. A. Global estimates of undiagnosed diabetes in adults. *Diabetes Res. Clin. Pract.* **103**, 150–160. https://doi.org/10.1016/j.diabres.2013.11.001 (2014).
5. Reaven, G. M. Banting lecture 1988. Role of insulin resistance in human disease. *Diabetes* **37**, 1595–1607. https://doi.org/10.2337/diab.37.12.15953 (1988).
6. Brownlee, M. Biochemistry and molecular cell biology of diabetic complications. *Nature* **414**, 813–820. https://doi.org/10.1038/414813a (2001).
7. Kahn, S. E., Hull, R. L. & Utzschneider, K. M. Mechanisms linking obesity to insulin resistance and type 2 diabetes. *Nature* **444**, 840–846. https://doi.org/10.1038/nature05482 (2006).
8. Premilovac, D. et al. Muscle insulin resistance resulting from impaired microvascular insulin sensitivity in Sprague Dawley rats. *Cardiovasc. Res.* **98**, 28–36. https://doi.org/10.1093/cvr/cvt015 (2013).
9. Stott, N. L. & Marino, J. S. High fat rodent models of type 2 diabetes: from rodent to human. *Nutrients* https://doi.org/10.3390/nu12123650 (2020).
10. Kleinert, M. et al. Animal models of obesity and diabetes mellitus. *Nat. Rev. Endocrinol.* **14**, 140–162. https://doi.org/10.1038/nrendo.2017.161 (2018).
11. Wang, Z. & Gleichmann, H. GLUT2 in pancreatic islets: Crucial target molecule in diabetes induced with multiple low doses of streptozotocin in mice. *Diabetes* **47**, 50–56. https://doi.org/10.2337/diab.47.1.50 (1998).
12. Reed, M. J. et al. A new rat model of type 2 diabetes: The fat-fed, streptozotocin-treated rat. *Metabol. Clin. Exper.* **49**, 1390–1394. https://doi.org/10.1053/meta.2000.17721 (2000).
13. Srinivasan, K., Viswanad, B., Asrat, L., Kaul, C. L. & Ramarao, P. Combination of high-fat diet-fed and low-dose streptozotocin-treated rat: A model for type 2 diabetes and pharmacological screening. *Pharmacol. Res.* **52**, 313–320. https://doi.org/10.1016/j.phrs.2005.05.004 (2005).
14. Srinivasan, K. & Ramarao, P. Animal models in type 2 diabetes research: An overview. *Indian J. Med. Res.* **125**, 451–472 (2007).
15. Podell, B. K. et al. A model of type 2 diabetes in the guinea pig using sequential diet-induced glucose intolerance and streptozotocin treatment. *Dis. Models Mech.* **10**, 151–162. https://doi.org/10.1242/dmm.025593 (2017).
16. Stranahan, A. M. et al. Diabetes impairs hippocampal function through glucocorticoid-mediated effects on new and mature neurons. *Nat. Neurosci.* **11**, 309–317. https://doi.org/10.1038/nn2055 (2008).
17. Kleinridders, A., Ferris, H. A., Cai, W. & Kahn, C. R. Insulin action in brain regulates systemic metabolism and brain function. *Diabetes* **63**, 2232–2243. https://doi.org/10.2337/db14-0568 (2014).
18. Deeds, M. C. et al. Single dose streptozotocin-induced diabetes: considerations for study design in islet transplantation models. *Lab. Animals* **45**, 131–140. https://doi.org/10.1258/la.2010.010090 (2011).
19. Graham, M. L., Janecek, J. L., Kittredge, J. A., Hering, B. J. & Schuurman, H. J. The streptozotocin-induced diabetic nude mouse model: Differences between animals from different sources. *Comparat. Med.* **61**, 356–360 (2011).
20. Hayashi, K., Kojima, R. & Ito, M. Strain differences in the diabetogenic activity of streptozotocin in mice. *Biol. Pharmaceut. Bullet.* **29**, 1110–1119. https://doi.org/10.1248/bpb.29.1110 (2006).
21. Zhang, M., Lv, X. Y., Li, J., Xu, Z. G. & Chen, L. The characterization of high-fat diet and multiple low-dose streptozotocin induced type 2 diabetes rat model. *Exper. Diabet. Res.* https://doi.org/10.1155/2008/704045 (2008).
22. Skovso, S. Modeling type 2 diabetes in rats using high fat diet and streptozotocin. *J. Diabet. Invest.* **5**, 349–358. https://doi.org/10.1111/jdi.12235 (2014).

23. Mansor, L. S. et al. Cardiac metabolism in a new rat model of type 2 diabetes using high-fat diet with low dose streptozotocin. *Cardiovascul. Diabetol.* **12**, 136. https://doi.org/10.1186/1475-2840-12-136 (2013).
24. Bonner-Weir, S. et al. Beta-cell growth and regeneration: replication is only part of the story. *Diabetes* **59**, 2340–2348. https://doi.org/10.2337/db10-0084 (2010).
25. Premilovac, D. et al. A new method for targeted and sustained induction of type 2 diabetes in Rodents. *Sci. Rep.* **7**, 14158. https://doi.org/10.1038/s41598-017-14114-4 (2017).
26. Southam, K. et al. Development and characterisation of a rat model that exhibits both metabolic dysfunction and neurodegeneration seen in type 2 diabetes. *J. Physiol.* **600**, 1611–1630. https://doi.org/10.1113/JP282454 (2022).
27. Daniel, A. et al. Novel short-chain quinones to treat vision loss in a rat model of diabetic retinopathy. *Int. J. Mol. Sci.* https://doi.org/10.3390/ijms22031016 (2021).
28. Attrill, E. et al. Metabolic-vascular coupling in skeletal muscle: A potential role for capillary pericytes?. *Clin. Exper. Pharmacol. Physiol.* **47**, 520–528. https://doi.org/10.1111/1440-1681.13208 (2020).
29. Parlee, S. D., Lentz, S. I., Mori, H. & Macdougald, O. A. 93–122 (Elsevier, 2014).
30. Palomäki, V. A., Koivukangas, V., Meriläinen, S., Lehenkari, P. & Karttunen, T. J. A straightforward method for adipocyte size and count analysis using open-source software QuPath. *Adipocyte* **11**, 99–107. https://doi.org/10.1080/21623945.2022.2027610 (2022).
31. Mehlem, A., Hagberg, C. E., Muhl, L., Eriksson, U. & Falkevall, A. Imaging of neutral lipids by oil red O for analyzing the metabolic status in health and disease. *Nat. Prot.* **8**, 1149–1154. https://doi.org/10.1038/nprot.2013.055 (2013).
32. Keske, M. A., Clerk, L. H., Price, W. J., Jahn, L. A. & Barrett, E. J. Obesity blunts microvascular recruitment in human forearm muscle after a mixed meal. *Diabet. Care* **32**, 1672–1677. https://doi.org/10.2337/dc09-0206 (2009).
33. Lenzen, S. The mechanisms of alloxan- and streptozotocin-induced diabetes. *Diabetologia* **51**, 216–226. https://doi.org/10.1007/s00125-007-0886-7 (2008).
34. Elsner, M., Tiedge, M., Guldbakke, B., Munday, R. & Lenzen, S. Importance of the GLUT2 glucose transporter for pancreatic beta cell toxicity of alloxan. *Diabetologia* **45**, 1542–1549. https://doi.org/10.1007/s00125-002-0955-x3 (2002).
35. Thorens, B. GLUT2, glucose sensing and glucose homeostasis. *Diabetologia* **58**, 221–232. https://doi.org/10.1007/s00125-014-3451-1 (2015).
36. Goyal, S. N. et al. Challenges and issues with streptozotocin-induced diabetes - A clinically relevant animal model to understand the diabetes pathogenesis and evaluate therapeutics. *Chem. Biol. Interact.* **244**, 49–63. https://doi.org/10.1016/j.cbi.2015.11.032 (2016).
37. Wang, Z. H., Hsu, C. C., Lin, H. H. & Chen, J. H. Antidiabetic effects of carassius auratus complex formula in high fat diet combined streptozotocin-induced diabetic mice. *Evid.-Based Compl. Alternat. Med.* https://doi.org/10.1155/2014/628473 (2014).
38. Tang, Y. et al. Optimization of streptozotocin dosing for establishing tumor-bearing diabetic mouse models. *J. South. Med. Univer.* **34**, 827–831 (2014).
39. de la Garza-Rodea, A. S., Knaän-Shanzer, S., den Hartigh, J. D., Verhaegen, A. P. & van Bekkum, D. W. Anomer-equilibrated streptozotocin solution for the induction of experimental diabetes in mice (Mus musculus). *J. Am. Assoc. Lab. Animal Sci.: JAALAS* **49**, 40–44 (2010).
40. Kamli-Salino, S. E. J. et al. Induction of experimental diabetes and diabetic nephropathy using anomer-equilibrated streptozotocin in male C57Bl/6J mice. *Biochem. Biophys. Res. Commun.* **650**, 109–116. https://doi.org/10.1016/j.bbrc.2023.01.089 (2023).
41. Bloch, K. et al. Improved activity of streptozotocin-selected insulinoma cells following microencapsulation and transplantation into diabetic mice. *Cell Biol. Int.* **30**, 138–143. https://doi.org/10.1016/j.cellbi.2005.08.012 (2006).
42. Prescott, M. J. & Lidster, K. Improving quality of science through better animal welfare: the NC3Rs strategy. *Lab. Anim. (NY)* **46**, 152–156. https://doi.org/10.1038/laban.1217 (2017).
43. Kennedy, A. J., Ellacott, K. L., King, V. L. & Hasty, A. H. Mouse models of the metabolic syndrome. *Dis. Model. Mech.* **3**, 156–166. https://doi.org/10.1242/dmm.003467 (2010).
44. Genuth, S. M., Przybylski, R. J. & Rosenberg, D. M. Insulin resistance in genetically obese, hyperglycemic mice. *Endocrinology* **88**, 1230–1238. https://doi.org/10.1210/endo-88-5-1230 (1971).
45. Coleman, D. L. Obese and diabetes: Two mutant genes causing diabetes-obesity syndromes in mice. *Diabetologia* **14**, 141–148. https://doi.org/10.1007/BF00429772 (1978).
46. Dixit, V. D. et al. Ghrelin inhibits leptin- and activation-induced proinflammatory cytokine expression by human monocytes and T cells. *J. Clin. Invest.* **114**, 57–66. https://doi.org/10.1172/jci21134 (2004).
47. Kratofil, R. M. et al. A monocyte–leptin–angiogenesis pathway critical for repair post-infection. *Nature* **609**, 166–173. https://doi.org/10.1038/s41586-022-05044-x (2022).
48. McPherson, N. O. & Lane, M. Male obesity and subfertility, is it really about increased adiposity?. *Asian J. Androl.* **17**, 450–458. https://doi.org/10.4103/1008-682x.148076 (2015).
49. Mounzih, K., Lu, R. & Chehab, F. F. Leptin treatment rescues the sterility of genetically obese ob/ob males. *Endocrinology* **138**, 1190–1193. https://doi.org/10.1210/endo.138.3.5024 (1997).
50. Ritskes-Hoitinga, M., Tobin, G., Jensen, T. L. & Mikkelsen, L. F. in *The Laboratory Mouse (Second Edition)* (ed Hans J. Hedrich) Ch. 4.3, 567–599 (Academic Press, 2012).
51. Dittmann, A. et al. High-fat diet in a mouse insulin-resistant model induces widespread rewiring of the phosphotyrosine signaling network. *Mol. Syst. Biol.* **15**, e8849. https://doi.org/10.15252/msb.20198849 (2019).
52. Hariri, N. & Thibault, L. High-fat diet-induced obesity in animal models. *Nutrit. Res. Rev.* **23**, 270–299. https://doi.org/10.1017/S0954422410000168 (2010).
53. Surwit, R. S., Kuhn, C. M., Cochrane, C., McCubbin, J. A. & Feinglos, M. N. Diet-induced type II diabetes in C57BL/6J mice. *Diabetes* **37**, 1163–1167. https://doi.org/10.2337/diab.37.9.1163 (1988).
54. Bradley, E. A. et al. Metformin improves vascular and metabolic insulin action in insulin-resistant muscle. *J. Endocrinol.* **243**, 85–96. https://doi.org/10.1530/JOE-19-0067 (2019).

Author contributions

All experiments were performed at the Medical Sciences Precinct, University of Tasmania. EA and DP conceived and designed the study. EA and SP performed the in vivo experiments. NS and SM performed the pancreas histology. EA and OS performed the liver and adipose histology. EA analysed all data collected and prepared the figures. EA, OS, NS, SP, SM, RR, SR, BS and DP interpreted the results. EA drafted the manuscript. EA, OS, NS, SP, SM, RR, SR, BS and DP revised the manuscript, provided intellectual feedback, and approved the final manuscript. All authors agree to be accountable for all aspects of the work, ensuring the accuracy and integrity of the work. All persons designated as authors qualify for authorship, and all those who qualify for authorship are listed.

Funding

This research was supported by the University of Tasmania, College of Health and Medicine Research Enhancement Program grant awarded to DP and BAS.

Declarations

Competing interests
The authors declare that they have no conflict of interest.

Additional information
Supplementary Information The online version contains supplementary material available at https://doi.org/10.1038/s41598-025-89162-2.

Correspondence and requests for materials should be addressed to D.P.

Reprints and permissions information is available at www.nature.com/reprints.

Publisher's note Springer Nature remains neutral with regard to jurisdictional claims in published maps and institutional affiliations.